Mechanics of Materials 11 (1991) 163-175 Elsevier

Static and dynamic axial loading of a partially debonded fiber

Andrew Norris and Yang Yang

Department of Mechanics and Materials Science, Rutgers University, Piscataway, NJ 08855-0909, USA

Received 16 May 1990; revised version received 29 October 1990

The stresses on a partially bonded fiber in a composite material subject to axial loads are derived for both static and dynamic conditions. The static stress intensity is calculated for a fiber which is only partially bonded circumferentially and subject to a constant axial stress gradient, i.e. a uniform axial body force. The same configuration of a single partially bonded fiber is then considered for loading in the form of a dynamic stress gradient in the fiber, and particular attention is given to the stress intensity factor at the edge of the bond when the fiber is subject to a step load. The numerical results show that the dynamic stress always overshoots the static value, and the time taken to achieve the static equilibrium stress can be quite long if the fiber is nearly debonded. This is related to the phenomenon that a very loosely bonded fiber may resonate strongly at a frequency which goes to zero as the size of the bond vanishes.

1. Introduction

A major cause of failure in fiber-reinforced composite materials is the phenomenon of fiber pull-out, particularly for composites containing short fibers and also when the fiber-matrix cohesion is insufficiently secure. The onset of pull-out may be due to transverse cracking through the matrix, resulting in a sudden transfer of load to the fibers as the crack passes. This and other mechanisms have been studied in detail by many researchers using theories of steadily increasing sophistication; for instance, Cox (1952), Aveston, Cooper and Kelly (1971), Budiansky et al. (1986), Gao et al. (1988), Sigl and Evans (1989), and McCartney (1989). These and other studies of pull-out have focused on purely static models, with a natural emphasis upon determining critical parameters such as the energy release rate for a debonded fiber, and the stress intensity factors for different fracture mechanisms. Little consideration has been given to the dynamic and inertial aspects of pull-out, which may be of some importance in very fast loading situations, such as when a transverse crack is rapidly tearing the composite.

In that case the transfer of stress onto the fibers could occur on time scales short enough that inertial effects are significant. Dynamic effects may also play a part in the failure of composites under other conditions, as in the passage of a mechanical—thermal shock wave.

In this paper we consider a simplified model of a single fiber which is only partially bonded in the sense depicted in Fig. 1, i.e. the configuration is uniform in the axial direction but varies circumferentially. The fiber is bonded over part of the 360° interface and debonded over the remaining part. In contrast, a fiber under pull-out conditions is expected to be bonded or debonded depending upon the position along the fiber, with axial symmetry about the fiber axis. We focus on the the circumferential debonding configuration since it is amenable to analysis for both static and dynamic loading and the explicit expressions derived here may shed some light on the much more difficult issue of dynamic pull-out. Furthermore, even though axial debonding along the length of the fiber is certainly more significant in terms of the failure of the composite, it will generally be preceded by some circumferential debonding de-

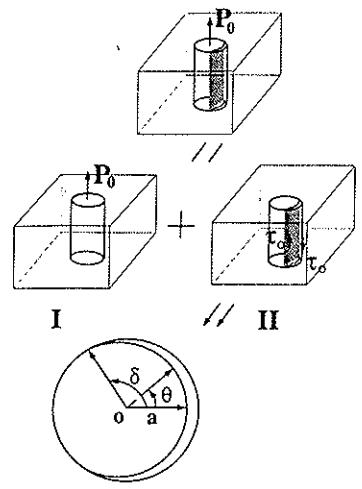


Fig. 1. The single fiber configuration and decomposition of the static problem for a debonded fiber.

pending upon the degree of axial symmetry prevailing initially. The results of this study are directly relevant to this precursor of the axial fiber pull-out.

The objective of this paper is to describe the transient loading of a single fiber which is partially bonded in the sense described above. We begin in Section 2 with an examination of the shear stress in a partially debonded fiber subject to a static axial body force. This material is necessary for purposes of comparison with the dynamic problem of Section 3 in which we consider a transient body force acting on a similarly debonded fiber. In particular, the long time response of a step load should be exactly the static response. The static results of Section 2 are of some interest in themselves, independent of the dynamic problem. For instance, it is shown that the static stress intensity factor at the edges of the debond is independent of the material mismatch for a given body force, and it becomes infinite in the limit as the fiber is almost completely debonded. We note that the force which governs the stress transfer to the matrix in both the static and dynamic problems is equivalent to an applied stress gradient in the fiber. The precise genesis of this dynamic body force is not discussed here, but it could originate from fast fracture of the matrix or shock wave loading. The assumptions involved in both the static and dynamic loadings considered in this paper are explained further in the discussion in Section 4.

2. The static problem for a debonded fiber

2.1. Formulation and decomposition of the problem

We first consider the static problem of a partially debonded fiber subject to a uniform axial body force P_0 per unit length. The loading P_0 may be considered as a locally uniform approximant to the imposed nonuniform force $\partial \sigma_{zz}^{f}/\partial z$, where z is the axial coordinate and σ_{zz}^f is the average axial stress in the fiber. The force P_0 is assumed to act uniformly inside the fiber which is partially bonded to the surrounding infinite matrix. The assumption of an infinite matrix simplifies the analysis, and all quantities are assumed independent of the axial coordinate, including the debond. The problem is therefore one of two-dimensional anti-plane strain for the configuration shown in Fig. 1. The extent of the circumferential debond is defined by the half angle δ , $0 < \delta < \pi$, subtended at the center of the fiber.

We first decompose the problem as indicated in Fig. 1, where I corresponds to a perfectly bonded fiber with the body force acting on the fiber, and in II shear tractions are applied over the debond which cancel those of I. Let u_f and u_m be the anti-plane displacements in the direction of the load P_0 , i.e. in the positive z-direction, then the solution to I is radially symmetric and easily determined as

$$u_{\rm f}^{(1)}(r) = \frac{P_0}{4\pi a^2 \mu_{\rm f}} (a^2 - r^2), \quad r < a, \tag{1}$$

$$u_{\rm m}^{(1)}(r) = \frac{-P_0}{2\pi\mu_m}\log(\frac{r}{a}), \qquad r > a.$$
 (2)

The solution to I of course requires that an equal but opposite load P_0 is applied to the matrix at infinity, and the rigid body displacement is chosen so that $u_f^{(1)}(a) = u_m^{(1)}(a) = 0$. The shear stress at the interface r = a is $\sigma_{rz}^{(1)} = \sigma_{rz}^{m(1)} = -\tau_0$, where

$$\tau_0 = \frac{P_0}{2\pi a},\tag{3}$$

(13)

and this provides the tractions necessary for problem II, see Fig. 1.

In problem II, both the fiber and matrix are free of body forces and the displacements satisfy the 2D Laplace equation. Standard methods for two-dimensional elasticity problems can then be used (Tamate and Yamada, 1969; England, 1976). Let u denote either of $u_i^{(II)}$ or $u_m^{(II)}$, then u(x, y)may be expressed in terms of a single complex-valued function $\phi(z)$, of the complex variable (not to be confused with the axial coordinate) z = x + iy $= r e^{i\theta}$

$$u = \frac{1}{2} \left[\phi(z) + \overline{\phi(z)} \right], \tag{4}$$

where the overbar denotes the complex conjugate, and the associated stress is

$$\sigma_{rz} - i\sigma_{\theta z} = \mu \phi'(z) \cdot e^{i\theta}. \tag{5}$$

Let ϕ_f , ϕ_m be the corresponding complex functions in the fiber and matrix, and let C denote the crack or debond, $-\delta < \theta < \delta$, and B the remaining bonded part of the interface, $|\theta| > \delta$. The boundary conditions are then: on the crack face $\sigma_{rz}^{f(11)} = \sigma_{rz}^{m(11)} = \tau_0$, or

$$\alpha \phi_{\rm f}'(\alpha) + \overline{\alpha} \overline{\phi_{\rm f}'(\alpha)} = 2a \frac{\tau_0}{\mu_{\rm f}}, \text{ on C}$$

$$\alpha \phi_{\rm m}'(\alpha) + \overline{\alpha} \overline{\phi_{\rm m}'(\alpha)} = 2a \frac{\tau_0}{\mu_{\rm m}}, \text{ on C}, \tag{6}$$

and on the bonded interface, both the stress and displacements are continuous.

$$\mu_{f} \left[\alpha \phi_{f}(\alpha) + \overline{\alpha} \overline{\phi'_{f}(\alpha)} \right] = \mu_{m} \left[\alpha \phi'_{m}(\alpha) + \overline{\alpha} \overline{\phi'_{m}(\alpha)} \right],$$
on B, (7)

$$\alpha \phi_{\rm f}'(\alpha) - \overline{\alpha} \overline{\phi_{\rm f}'(\alpha)} = \alpha \phi_{\rm m}'(\alpha) - \overline{\alpha} \overline{\phi_{\rm m}'(\alpha)}, \text{ on B,}$$
(8)

where

$$\alpha = a e^{i\theta}. (9)$$

The inhomogeneous equations (6) may be made homogeneous by the introduction of new functions $\psi_f(z)$ and $\psi_m(z)$ defined by

$$\phi'_{\rm f}(z) = \psi'_{\rm f}(z) + \frac{a\tau_0}{z\mu_{\rm f}}, \quad \phi'_{\rm m}(z) = \psi'_{\rm m}(z) + \frac{a\tau_0}{z\mu_{\rm m}}.$$
(10)

Thus, the boundary conditions at the crack face

$$a\psi'_{f}(\alpha) + \overline{\alpha}\overline{\psi'_{f}(\alpha)} = 0, \quad \alpha\psi'_{m}(\alpha) + \overline{\alpha}\overline{\psi'_{m}(\alpha)} = 0,$$

on C, (11)

and the conditions (7) and (8) on the bonded interface are now

$$\mu_{f} \left[\alpha \psi_{f}'(\alpha) + \overline{\alpha} \overline{\psi_{f}'(\alpha)} \right]$$

$$- \mu_{m} \left[\alpha \psi_{m}'(\alpha) + \overline{\alpha} \overline{\psi_{m}'(\alpha)} \right] = 0, \text{ on B,}$$

$$\left[\alpha \psi_{f}'(\alpha) - \overline{\alpha} \overline{\psi_{f}'(\alpha)} \right]$$

$$- \left[\alpha \psi_{m}'(\alpha) - \overline{\alpha} \overline{\psi_{m}'(\alpha)} \right] = 0, \text{ on B.}$$

$$(13)$$

The function $\phi'_{i}(z)$ is holomorphic within the fiber region, |z| < a, and so $\psi'_f(z)$ is holomorphic in the same region, except at z = 0 where it possesses a simple pole. Both $\phi_{\rm m}'(z)$ and $\psi_{\rm m}'(z)$ are holomorphic in |z| > a. We note that the applied tractions of problem II are self-equilibrated, hence the stress must vanish at infinity like z^{-1} . The corresponding condition on $\phi'_m(z)$ is

$$\psi'_{\rm m}(z) = \frac{-a\tau_0}{z\mu_{\rm m}} + O(z^{-2}), \quad |z| \to \infty.$$
 (14)

Finally, the stress at the center of the fiber must be bounded, implying

$$\psi_{\rm f}'(z) = \frac{-a\tau_0}{z\mu_f} + O(1), \quad |z| \to 0.$$
 (15)

2.2. Solution of problem II

Introduce new functions $\gamma'_{f}(z)$ and $\gamma'_{m}(z)$ de-

$$\gamma_{\mathbf{f}}'(z) = z\psi_{\mathbf{f}}'(z), \quad |z| < a, \tag{16}$$

$$\gamma_{\rm m}'(z) = z\psi_{\rm m}'(z), \quad |z| > a. \tag{17}$$

Although these stress functions have meaning only in their respective regions |z| < a and |z|> a, respectively, it is useful to analytically continue them into their complementary regions according to

$$\gamma_{\rm f}'(z) = -\frac{a^2}{z} \overline{\psi_{\rm f}'\left(\frac{a^2}{\overline{z}}\right)}, \quad |z| > a, \tag{18}$$

$$\gamma'_{\rm m}(z) = -\frac{a^2}{z} \overline{\psi'_{\rm m}\left(\frac{a^2}{\overline{z}}\right)}, \quad |z| < a.$$
 (19)

Thus, for any z, except possibly |z| = a,

$$\gamma_{\rm f}'\left(\frac{a^2}{\overline{z}}\right) = -\overline{\gamma_{\rm f}'(z)}, \quad \gamma_{\rm m}'\left(\frac{a^2}{\overline{z}}\right) = -\overline{\gamma_{\rm m}'(z)}.$$
 (20)

Let ${\gamma_i'}^+(\alpha)$ and ${\gamma_i'}^-(\alpha)$ be the limiting values of ${\gamma_i'}(z)$ as z approaches $\alpha = a e^{i\theta}$ from |z| < a and |z| > a, respectively, with similar definitions for ${\gamma_m'}^+(\alpha)$ and ${\gamma_m'}^-(\alpha)$. Then the boundary conditions (11) become

$$\gamma_{f}^{\prime +}(\alpha) - \gamma_{f}^{\prime -}(\alpha) = 0, \text{ on } C$$

$$\gamma_{m}^{\prime +}(\alpha) - \gamma_{m}^{\prime -}(\alpha) = 0, \text{ on } C,$$
 (21)

which means that $\gamma_f'(z)$ and $\gamma_m'(z)$ are continuous across the crack. The remaining interface conditions (12) and (13) become

$$[\mu_{f}\gamma_{f}^{\prime +}(\alpha) + \mu_{m}\gamma_{m}^{\prime +}(\alpha)]$$

$$- [\mu_{f}\gamma_{f}^{\prime -}(\alpha) + \mu_{m}\gamma_{m}^{\prime -}(\alpha)] = 0, \text{ on B,}$$

$$[\gamma_{f}^{\prime +}(\alpha) - \gamma_{m}^{\prime +}(\alpha)]$$

$$+ [\gamma_{f}^{\prime -}(\alpha) - \gamma_{m}^{\prime -}(\alpha)] = 0, \text{ on B.}$$

$$(23)$$

Thus, $\gamma'_f(z)$ and $\gamma'_m(z)$ are holomorphic everywhere except across the bonded interface B. Their behavior at the origin and infinity is

$$\mu_{\rm f} \gamma_{\rm f}' = -\mu_{\rm m} \gamma_{\rm m}' = \begin{cases} -a \tau_0, & z \to 0, \\ a \tau_0, & z \to \infty. \end{cases}$$
 (24)

Using Cauchy's theorem, the unique solution to (22) that also satisfies Eqs. (21) and (24) follows as

$$\mu_f \gamma_f'(z) + \mu_m \gamma_m'(z) = 0, \quad \text{for all } z. \tag{25}$$

It remains to determine the function

$$h(z) = \gamma_{\rm f}'(z) - \gamma_{\rm m}'(z), \tag{26}$$

which from (23) satisfies

$$h^{+}(\alpha) + h^{-}(\alpha) = 0$$
, on B. (27)

This is a homogeneous Hilbert problem, with the extra conditions from (24),

$$-h(0) = h(\infty) = a\tau_0 \frac{\mu_f + \mu_m}{\mu_f \mu_m}.$$
 (28)

The solution for h(z) is

$$h(z) = (c_0 + c_1 z) \chi(z),$$
 (29)

where c_0 , c_1 are constants and

$$\chi(z) = (z - a e^{-i\delta})^{-1/2} (z - a e^{i\delta})^{-1/2}.$$
 (30)

The function $\chi(z)$ is single-valued everywhere except along the bonded interface B. The constants c_0 and c_1 then follow from the two conditions in (28) as

$$c_0 = ah(0), \quad c_1 = h(\infty).$$
 (31)

Combining (25), (26), (28), (29) and (31) yields

$$\gamma_{\rm f}'(z) = \frac{a\tau_0}{\mu_{\rm f}}(z-a) \ \chi(z),$$

$$\gamma_{\rm m}'(z) = \frac{-a\tau_0}{\mu_{\rm m}}(z-a) \ \chi(z). \tag{32}$$

This completes the solution to problem II.

2.3. Stress intensity on the static debond

The total static shear stress $\sigma_{rz}^{f}(a, \theta) = \sigma_{rz}^{m}(a, \theta) \equiv \sigma_{rz}^{s}(\theta)$ along the bonded interface follows from the separate solutions to problems I and II as

$$\sigma_{rz}^{s}(\theta) = \frac{\mu_{f}}{2a} \left[\gamma_{f}^{\prime +}(\alpha) - \gamma_{f}^{\prime -}(\alpha) \right], \quad \text{on B.}$$
 (33)

Use of (30) and (32) gives the explicit result

$$\sigma_{rx}^{s}(\theta) = \frac{-\tau_{0} \sin(\frac{1}{2}\theta)}{\sqrt{\sin[\frac{1}{2}(\theta + \delta)] \sin[\frac{1}{2}(\theta - \delta)]}}, \text{ on B.}$$
(34)

The condition that the fiber is subject to zero net force implies

$$\int_{\varepsilon}^{\pi} \sigma_{rz}^{s}(\theta) d\theta = -\pi \tau_{0}, \qquad (35)$$

and it may be shown by direct integration that (34) satisfies this. Furthermore, we note that $\sigma_{rz}^s(\theta)$ is independent of the material mismatch characterized by the ratio μ_t/μ_m , i.e. the stress on the bonded neck due to the interior body force $P_0 = 2\pi a \tau_0$ per unit axial length is the same whatever the fiber-matrix combination. The stress intensity factor K_s is defined as

$$K_{s} = \lim_{\theta \to \delta^{+}} \left[a(\theta - \delta) \right]^{1/2} \sigma_{rz}^{s}(\theta), \tag{36}$$

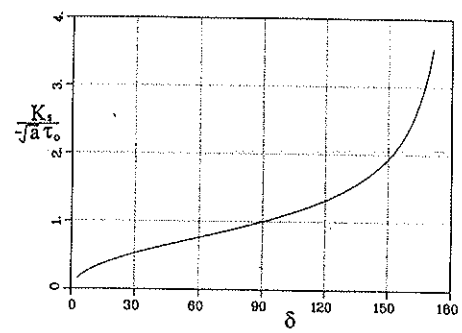


Fig. 2. Stress intensity factor for a debonded fiber under a static load.

and therefore

$$\frac{K_{\rm s}}{-\tau_0\sqrt{a}} = \left[\tan\left(\frac{1}{2}\delta\right)\right]^{1/2}.\tag{37}$$

The simplicity of this expression is noteworthy, as is the fact that the stress intensity factor is the same for all material combinations. Also, K_s becomes infinite as $\delta \to \pi$, see Fig. 2, which is not surprising since in this limit the vanishingly thin neck must support a finite load. The monotonically increasing nature of K_s as a function of δ means that any crack propagation instability will lead to catastrophic crack growth and complete debonding in the circumferential direction. It is important to point out that this does not occur if the fiber is subject to a remote loading in the matrix. Karihaloo and Viswanathan (1985) considered the response of an elliptical fiber under remote shear loading and their results predict a finite mode III stress intensity factor in the limit as the fiber becomes completely debonded.

3. Dynamic loading of an isolated fiber

3.1. Formulation of the dynamic problem

We now extend the two-dimensional static solution of the previous section to the dynamic case. Thus, the debond is again circumferential, as illustrated in Fig. 1, with no variation in the axial direction. This is of course an approximation, but it should be valid for fibers with relatively constant debonds extending over an axial distance of

many fiber radii. The loading on the fiber is also assumed independent of the axial coordinate, and is in the form of a causal time-dependent axial stress gradient P(t), such that P(t) = 0 for t < 0. Thus, P(t) corresponds to a dynamic generalization of the static load P_0 of the previous section.

Define the Fourier transform pair for any causal quantity g(t) as

$$\hat{g}(\omega) = \int_0^\infty g(t) e^{i\omega t} dt,$$

$$g(t) = \frac{1}{\pi} \text{Re} \int_0^\infty \hat{g}(\omega) e^{-i\omega t} d\omega.$$
(38)

We seek solutions for the time harmonic displacement fields $\hat{u}_t(r, \theta, \omega)$ and $\hat{u}_m(r, \theta, \omega)$ in the fiber and matrix respectively. The equations of motion are

$$\nabla^2 \hat{u}_{\rm f} + k_{\rm f}^2 \hat{u}_{\rm f} + \frac{\hat{P}(\omega)}{\pi a^2 \mu_{\rm f}} = 0, \quad r < a, \tag{39}$$

$$\nabla^2 \hat{u}_{\rm m} + k_{\rm m}^2 \hat{u}_{\rm m} = 0, \qquad r > a, \tag{40}$$

where $k_{\rm f} = \omega (\rho_{\rm f}/\mu_{\rm f})^{1/2}$, $k_{\rm m} = \omega (\rho_{\rm m}/\mu_{\rm m})^{1/2}$ and $\rho_{\rm f}$ and $\rho_{\rm m}$ are the volumetric densities. The general solutions to Eqs. (39) and (40) that are bounded for r > a and satisfy the radiation condition for r > a, are

$$\hat{u}_{f}(r, \theta, \omega) = \frac{-\hat{P}(\omega)}{\pi \mu_{f}(k_{f}a)^{2}} + \sum_{n=0}^{\infty} F_{n}J_{n}(k_{f}r) \cos n\theta, \qquad (41)$$

$$\hat{u}_{\rm m}(r,\,\theta,\,\omega) = \sum_{n=0}^{\infty} E_n H_n^{(1)}(k_{\rm m}r) \cos n\theta, \qquad (42)$$

where J_n and $H_n^{(1)}$ are Bessel and Hankel functions of order n and E_n and F_n are frequency-dependent constants. The stress must be continuous over the entire interface

$$u_{\rm f} \frac{\partial \hat{u}_{\rm f}}{\partial r} = \mu_{\rm m} \frac{\partial \hat{u}_{\rm m}}{\partial r}, \quad r = a, -\pi < \theta < \pi,$$
 (43)

and therefore.

$$E_{n} = \frac{\rho_{f}}{\rho_{m}} \frac{k_{m}}{k_{f}} \frac{J_{n}'(k_{f}a)}{H_{n}'^{(1)'}(k_{m}a)} F_{n}, \quad n = 0, 1, 2, \dots$$
(44)

Let the unknown stress on the bonded interface B be $\hat{\tau}(\theta, \omega)$, then $\hat{\tau}$ is even in θ and

$$\mu_{\mathbf{f}} \frac{\partial \hat{u}_{\mathbf{f}}}{\partial r} = \begin{cases} 0, & 0 < \theta < \delta, \\ \hat{\tau}(\theta, \omega), & \delta < \theta < \pi. \end{cases}$$
(45)

Therefore,

$$F_{n} = \frac{\epsilon_{n}}{\pi \mu_{f} k_{f} J_{n}'(k_{f} a)} \int_{\delta}^{\pi} \hat{\tau}(\theta, \omega) \cos n\theta \, d\theta,$$

$$n = 0, 1, 2, ..., \tag{46}$$

where $\epsilon_0 = 1$, $\epsilon_n = 2$, for $n \ge 1$. The final condition is the continuity of displacement over the bonded interface, which along with Eqs. (42)-(45), implies

$$a \sum_{n=0}^{\infty} \epsilon_n \cos n\theta \ L_n \int_{\delta}^{\pi} \hat{\tau}(\theta', \omega) \cos n\theta' \ d\theta'$$
$$= \hat{P}(\omega), \quad \delta < \theta < \pi, \tag{47}$$

where

$$L_{n}(\omega) = k_{f} a \frac{J_{n}(k_{f} a)}{J'_{n}(k_{f} a)} - \frac{\rho_{f}}{\rho_{m}} k_{m} a \frac{H_{n}^{(1)}(k_{m} a)}{H_{n}^{(1)}(k_{m} a)}.$$
(48)

3.2. Dynamic stress on a bonded fiber

An explicit solution to the integral equation (47) may be obtained in the single case that the fiber is fully bonded ($\delta = 0$). The interface shear stress is then radially symmetric, $\hat{\tau}(\theta, \omega) = \hat{\tau}(\omega)$, and

$$\hat{\tau}(\omega) = \frac{\hat{P}(\omega)}{\pi a L_0(\omega)}.$$
 (49)

We consider specifically the step load

$$P(t) = P_0 H(t), \tag{50}$$

where H(t) = 0, $t \le 0$, H(t) = 1, t > 0, is the Heaviside function, and P_0 is a constant. The natural unit for the dynamic stress $\tau(t)$ is τ_0 defined in (3). The long time behavior of $\tau(t)$ is governed by the zero-frequency component of $\hat{\tau}(\omega)$, which follows from (49) and (50) as $\hat{\tau}(\omega) = \tau_0/i\omega + O(1)$ as $\omega \to 0$, and is therefore just the

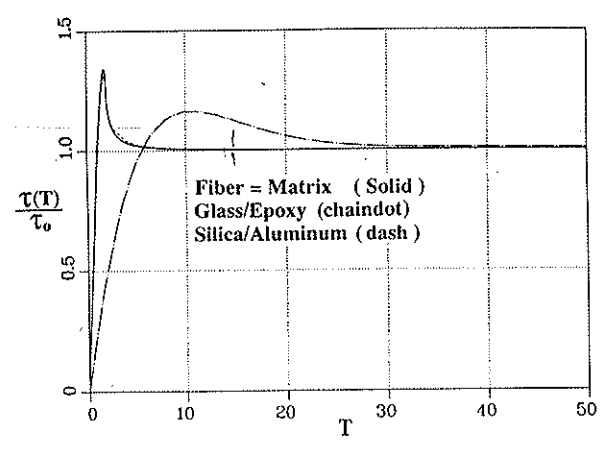


Fig. 3. The shear stress on a perfectly bonded fiber subjected to a step load at T=0, where $T=c_{\rm f}t/a$ is the dimensionless time, and $\tau_0=P_0/2\pi a$ is the static stress solution. The material parameters used are listed in Table 1.

simple static stress for a bonded fiber, i.e. $\tau(t) \rightarrow -\tau_0$ as $t \rightarrow \infty$. The transient stress is illustrated in Fig. 3 in terms of the dimensionless time

$$T = \frac{c_{\rm f}}{a}t, \quad c_{\rm f} = \sqrt{\mu_{\rm f}/\rho_{\rm f}}, \tag{51}$$

where $c_{\rm f}$ is the shear wave speed in the fiber. The response for a homogeneous medium is shown for comparison, and it is not much different from the response for silica/Al. Generally, the dynamic stress overshoots the static value before relaxing to the static equilibrium stress. The interval required to achieve the asymptotic static stress appears to increase if the fibers are much stiffer than the matrix, as illustrated by the response for glass/epoxy.

3.3. Solution of the dynamic problem

The presence of the debond can lead to stress concentrations at the crack tips $\theta = \delta$ and $\theta = -\delta$.

Table 1

Material	E (GN m ⁻²)	ν	$\rho (g/cm^3)$
Glass (fiber)	70.68	0.182	2.55
Epoxy (matrix)	3.22	0.258	1.25
Silica (fiber)	73	0.177	2.55
Aluminum (matrix)	70.5	0.345	2.7

The static solution of Section 2 indicates that the form of the singularity is at most of the inverse square root type. A static analysis of mode III fracture at an interface crack leads to the same conclusion, while dynamic analysis of the canonical problem of diffraction of a plane time harmonic SH wave from a semi-infinite crack between two materials (Clemmow, 1953) also shows that the singularity of stress is of inverse square root form. Thus, we do not have to deal with the complication of oscillating singularities common to in-plane fracture problems (Rice, 1988). Accordingly, we expand the stress as

$$\hat{\tau}(\theta, \omega) = \frac{\hat{P}(\omega)}{\pi a} \frac{1}{\sqrt{\epsilon^2 - (\pi - \theta)^2}} \times \sum_{n=0}^{\infty} \beta_n(\omega) \phi_n^{(s)}(\theta),$$
 (52)

where $\epsilon = \pi - \delta$ and $\phi_n^{(s)}$ are related to Chebyshev polynomials T_{2n} (Abramowitz and Stegun, 1965)

$$\phi_n^{(s)}(\theta) = (-1)^n T_{2n} \left(\frac{\pi - \theta}{\epsilon} \right)$$
$$= (-1)^n \cos \left(2n \arccos \frac{\pi - \theta}{\epsilon} \right). \tag{53}$$

These have the useful property that

$$\int_{\delta}^{\pi} \frac{\phi_n^{(s)}(\theta) \cos m\theta}{\sqrt{\epsilon^2 - (\pi - \theta)^2}} d\theta = (-1)^m \frac{\pi}{2} J_{2n}(m\epsilon).$$
 (54)

Taking appropriate inner products with eq. (47) yields an infinite system of equations for the stress coefficients β_n ,

$$\sum_{n=0}^{\infty} Q_{mn} \beta_n = \delta_{m0}, \quad m = 0, 1, 2, \dots,$$
 (55)

where Q_{mn} are complex-valued elements of an infinite, symmetric matrix,

$$Q_{mn}(\omega) = \frac{1}{2} L_0 \delta_{m0} \delta_{n0} + \sum_{p=1}^{\infty} L_p J_{2m}(p\epsilon) J_{2n}(p\epsilon).$$
(56)

In order to avoid an ill-conditioned system in the static limit discussed below, we eliminate β_0 using the equation for m = 0,

$$\beta_0 = \frac{1}{Q_{00}} - \sum_{n=1}^{\infty} Q_{0n} \beta_n, \tag{57}$$

and then solve the system

$$\sum_{n=1}^{\infty} \left(Q_{mn} - \frac{Q_{m0}Q_{n0}}{Q_{00}} \right) \beta_n = -\frac{Q_{m0}}{Q_{00}},$$

$$\vdots \qquad m = 1, 2, \dots$$
(58)

The coefficient $\beta_0(\omega)$ is related to the net force transmitted across the bonded neck, and it is shown in Appendix A that the total power lost into the matrix is proportional to $Im(\beta_0)$.

3.4. Comparison with the static solution

The asymptotic expansion for Q_{mn} in the static limit, $k_1 a \ll 1$, is

$$Q_{mn}(\omega) = -\delta_{m0}\delta_{n0} + \left(1 + \frac{\mu_{\rm f}}{\mu_{\rm m}}\right)(k_{\rm f}a)^{2}$$

$$\times \sum_{p=1}^{\infty} J_{2m}(p\epsilon) J_{2n}(p\epsilon) + O(k_{\rm f}a)^{3}.$$
(59)

Therefore, in this limit, $\beta_0 = -1 + O(k_f a)$, and the system of equations (58) for the other coefficients in the stress expansion becomes

$$\sum_{n=1}^{\infty} \hat{Q}_{mn} \beta_n(0) = \hat{Q}_{m0}, \quad m = 1, 2, \dots,$$
 (60)

where \hat{Q}_{mn} are real-valued matrix elements,

$$\hat{Q}_{mn} = \sum_{n=1}^{\infty} J_{2m}(p\epsilon) J_{2n}(p\epsilon).$$

The stress coefficients β_n , $0=1, 2, \ldots$, are therefore real and independent of the material constants, specifically the ratio μ_f/μ_m . These results correspond to the static findings of Section 3.3, in particular, $\lim_{\omega \to 0} 2\pi a \hat{\tau}(\theta, \omega)/\hat{P}(\omega)$ is exactly equal to $\sigma_{rz}^s(\theta)/\tau_0$. The fact that $\beta_0 \to -1$ is equivalent to the condition (35) for no net force on the fiber.

3.5. The dynamic stress intensity factor

The dynamic stress intensity factor is defined in the same manner as for the static problem,

$$\hat{K}_{d}(\omega) = \lim_{\theta \to \delta^{+}} \left[a(\theta - \delta) \right]^{1/2} \hat{\tau}(\theta, \omega)$$
$$= \frac{\hat{P}(\omega)}{2\pi a} \left(\frac{2a}{\epsilon} \right)^{1/2} \sum_{n=0}^{\infty} (-1)^{n} \beta_{n}(\omega), \quad (61)$$

In the static limit, we obtain

$$\frac{\hat{K}_{d}(0)}{\hat{\tau}_{0}\sqrt{a}} = \left(\frac{2}{\epsilon}\right)^{1/2} \sum_{n=1}^{\infty} (-1)^{n} \beta_{n}(0), \qquad (62)$$

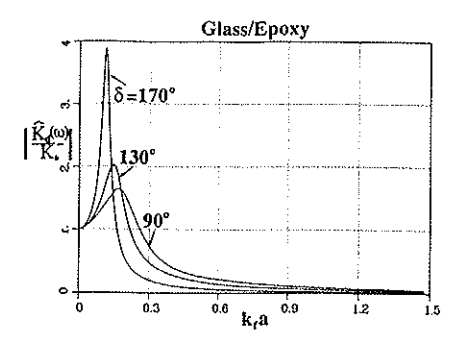
where $\beta_n(0)$ are determined from eq. (60), and

$$\hat{\tau}_0 = \frac{\hat{P}(0)}{2\pi a} \,. \tag{63}$$

The definition of $\hat{\tau}_0$ only makes sense, of course, when the zero-frequency component of the applied force is defined. This is not the case for the step load considered above, but it may be included by an appropriate extension of (63).

4. Numerical results and discussion

The ratio of the dynamic stress intensity factor to the static SIF is plotted in Fig. 4 as a function of frequency for different neck widths and different material combination. As expected, the ratio approaches unity as the dimensionless frequency



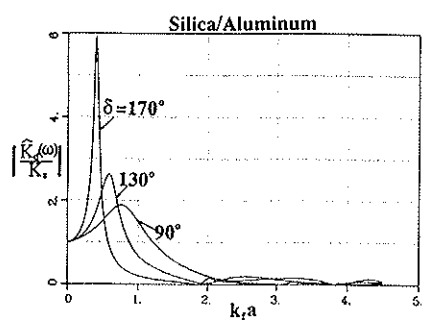
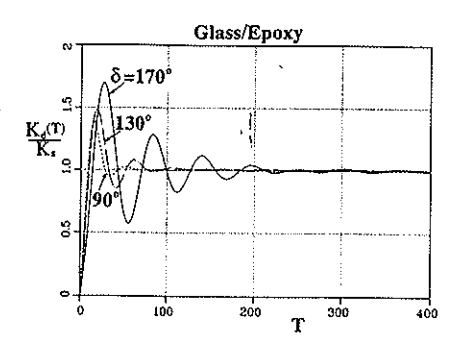


Fig. 4. The absolute value of the ratio of dynamic stress intensity to the static SIF versus nondimensional frequency $k_f a$ for different values of the crack semi-angle δ .



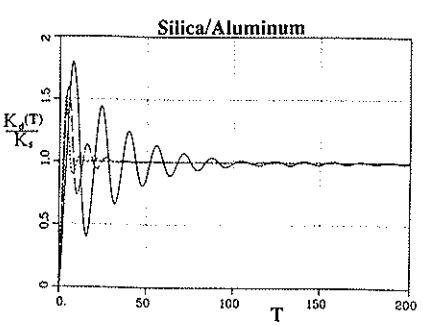


Fig. 5. The magnitude of the ratio of dynamic stress intensity to static SIF for a partially debonded fiber versus nondimensional time T. The load is a step function at T=0. The solid curves are for $\delta=170^{\circ}$, the chaindotted curves for $\delta=130^{\circ}$, and the dashed curves for $\delta=90^{\circ}$.

 $k_f a \rightarrow 0$. However, the dynamic SIFs in Fig. 4 clearly exhibit a resonance behavior, at a frequency that is small and decreases with ϵ . Fig. 5 shows the ratio of the dynamic SIF to the static SIF in the time domain for step loading. The dynamic SIFs not only overshoot the static SIFs but also ring exactly at their resonant frequencies shown in Fig. 4. In general, the smaller the neck, the longer the fiber will oscillate.

This resonance is essentially a rattling phenomenon that occurs when the fiber is almost completely disconnected from the matrix. It has been discussed and quantified by Yang and Norris (1990) and Norris and Yang (1990), who consider the related problem of SH wave scattering from a partially debonded fiber. The resonance may be understood as that of a spring mass system, where the spring constant is defined by the ability of the neck to transmit shear force between the matrix and fiber, and the mass is the inertia of the fiber. As the neck vanishes, i.e. as $\delta \to \pi$, the spring

stiffness goes to zero, but the inertia of the fiber remains unchanged. Therefore, the resonance frequency goes to zero in the limit as $\delta \to \pi$.

The form of the resonance is well described by the following asymptotic approximation. In the low frequency limit, the quasistatic approximation for the stress intensity factor discussed in Section 2 is not uniformly valid in ϵ as $\epsilon \to 0$. It can be shown, using the methods of Norris and Yang (1990), that $\beta_m = O(\epsilon^{2m-1})$, m > 0, if $k_f a$ is small and ϵ is also small. Therefore, the β_0 term will dominate Eq. (61) for the stress intensity in this double limit, i.e.

$$\hat{K}_{d}(\omega) = \frac{\hat{P}(\omega)}{2\pi a} \left(\frac{2a}{\epsilon}\right)^{1/2} \beta_{0}(\omega). \tag{64}$$

A double asymptotic expansion of Q_{00} for both $k_f a \ll 1$ and $\epsilon \ll 1$ yields (Norris and Yang, 1990)

$$\beta_{0}(\omega) \sim -\left\{1 - \frac{\mu_{f}}{\mu_{m}} (k_{f}a)^{2} \left[\left(1 + \frac{\mu_{m}}{\mu_{f}}\right) \Sigma(\epsilon) + \frac{\mu_{m}}{8\mu_{f}} - \frac{1}{2}\gamma - \frac{1}{2} \log(\frac{1}{2}k_{m}a) + \frac{1}{4}i\pi \right] \right\}^{-1}, \quad (65)$$

where

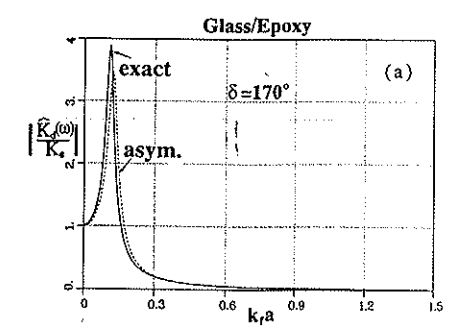
$$\Sigma(\epsilon) = \log\left(\frac{2}{\epsilon}\right) + \frac{1}{6}\epsilon^2 + O(\epsilon^4).$$

The asymptotic behavior of $\Sigma(\epsilon)$ as $\epsilon \to 0$ implies that the low frequency behavior of $\beta_0(\omega)$ can be quite different in character from the quasistatic approximation, $\beta_0 \sim -1$, valid only for $\epsilon = O(1)$. The resonant form of $\hat{K}_d(\omega)$ illustrated in Fig. 4 is thus due to the possibility that $\beta_0(\omega)$ can vary substantially from -1 even as $k_f a$ is small, if ϵ is also small. The resonant frequency predicted from eq. (65) is to first order

$$k_{\rm f}a = \left[\left(1 + \frac{\mu_{\rm f}}{\mu_{\rm m}} \right) \Sigma(\epsilon) \right]^{-1/2},\tag{66}$$

which is $O(1/\sqrt{\log |\epsilon|})$ as $\epsilon \to 0$.

The predictions based on Eqs. (64) and (65) are compared in Fig. 6 with the full, numerically intensive computations for the stress intensity factor in both the frequency and time domains. The agreement between them is remarkably good, and suggests that the simple form of the asymptotic



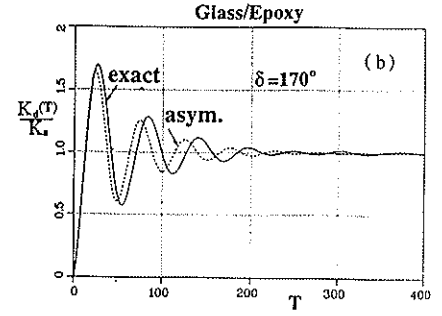


Fig. 6. (a) The absolute value of the ratio of dynamic stress intensity to static SIF versus nondimensional frequency $k_f a$ for glass/epoxy, $\delta = 170^{\circ}$. The solid curve is the result of the "exact" numerical calculations, the dashed curve follows from the asymptotic approximation of Eq. (65). (b) The corresponding ratio in the time domain versus nondimensional time T for a step load at T = 0.

approximation in Eqs. (64) and (65) can be used to describe the transient response of a loosely connected fiber. The approximation contains the correct static limit as $\omega \to 0$ and also captures the low frequency resonance phenomenon.

The frequency domain solution obtained here can easily be combined with the spectrum of an arbitrary excitation to yield the corresponding transient response. For instance, Fig. 7 illustrates dynamic SIF of a fiber subject to a forced excitation in the form of a narrow-band pulse of several cycles. The fiber is such that it is almost debonded, with $\delta = 170\,^{\circ}$, and the forcing frequency is equal to the resonant frequency, see Fig. 4. The forcing causes the magnitude of the dynamic stress intensity factor to achieve a value almost six times that of the static SIF in a few periods. This illustrates quite clearly how in certain circumstances the role of fiber inertia may not be ignored,

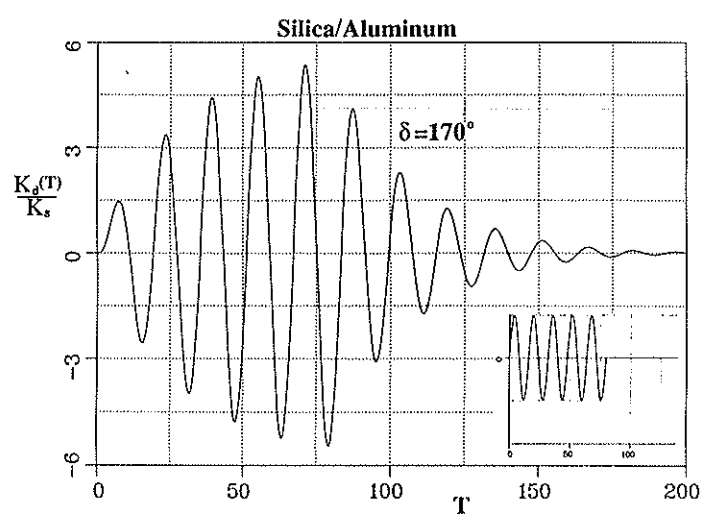


Fig. 7. The ratio of dynamic stress intensity to static SIF versus nondimensional time T for glass/epoxy under sinusoidal pulse loading with the period identical to the resonant period of the composite system, 15.9 in dimensionless time units. The precise form of the loading pulse is indicated in the insert.

and that purely dynamic effects can lead to transient stresses far in excess of those that would be estimated on the basis of static equilibrium.

Finally, we conclude with a brief discussion on the nature of the applied forces P_0 and P(t) of Sections 2 and 3. The force P_0 is equivalent to a uniform stress gradient $\partial \sigma_{zz}^f / \partial z$ in the fiber for all z. However, in practical situations the stress σ_{zz}^f cannot be a linear function of z, and therefore we should think of P_0 and P(t) as approximations to spatially varying functions. For instance, consider the composite cylinders model of pull-out loading depicted in Fig. 8 for a fiber which is fully bonded

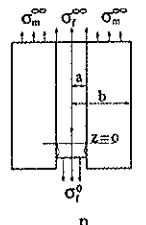




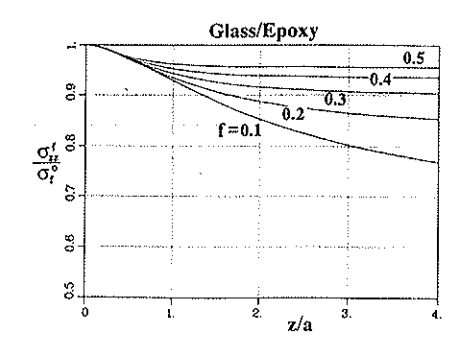
Fig. 8. A fiber under axial pull-out load in the composite cylinders model of a fiber reinforced material, and the load on a fiber traversing a matrix crack.

for z > 0 and detached from the matrix for z < 0. In this case it is possible to estimate the axial stress and its gradient in the bonded section z > 0 using a shear-lag theory (e.g. Cox, 1952; Budiansky et al., 1986; Sigl and Evans, 1989; McCartney, 1989). Based on the fourth-order theory of McCartney (1989), the following axial and shear stresses in the fiber are

$$\sigma_{zz}^{f}(z) = \sigma_{f}^{\infty} + S(z), \tag{67}$$

$$\sigma_{rz}^{f}(r,z) = \frac{1}{2}rS'(z), \tag{68}$$

where S(z) is defined in Appendix B. Note that the stress gradient is directly proportional to the shear stress. Representative stress distributions for this model are illustrated in Figs. 9 and 10. These results show that as one proceeds along a fiber away from the loaded end into the composite, the axial stress diminishes steadily, until it eventually assumes a constant value. In particular, significant stress gradients are confined to a region close to the fiber end being pulled, although the extent of this region can be several fiber radii. Also, the maximum shear stress tends to occur closer to the pulled end as the fiber volume fraction f increases. The two combinations of materials considered in Figs. 9 and 10 include one for which the material parameters are not much different



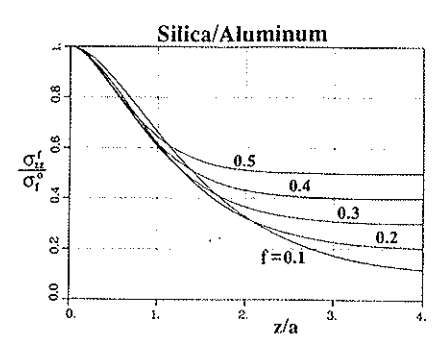
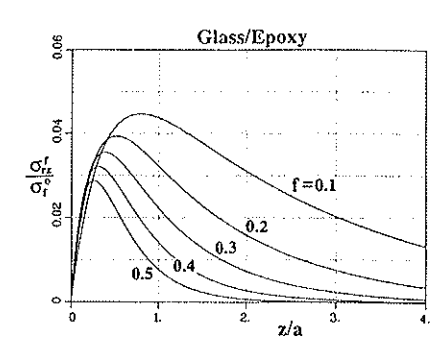


Fig. 9. The decay of the axial stress in a fiber.



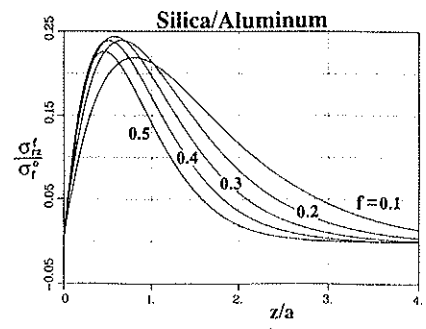


Fig. 10. The shear stress $\sigma_{rz}^f(a, z)$ at the interface of a fully bonded fiber subject to static pull-out.

(silica/Al), and one for which they differ significantly (glass/epoxy). The shear stress actually oscillates about zero for large values of z/a for silica/Al, although the magnitude of the oscillations are very small. The nondimensionalized shear stress for glass/epoxy is considerably less than for the silica/Al composite.

5. Conclusions

Results have been obtained for the static and dynamic loading of a circumferentially debonded fiber. The solution for the static problem is summarized by Eq. (34) for the interfacial stress between the matrix and the bonded segment of the fiber. The corresponding stress intensity factor, Eq. (37), increases without bound as the fiber debonds completely, indicating the likelihood of catastrophic cracking in the circumferential direction. The analysis for dynamic loading shows that the results of the static problem are obtained in the zero-frequency limit, or equivalently, in the long time response to a step load. For short times, i.e. nonzero frequencies, the dynamic stress intensity factor always overshoots the static value. Departures from the static limit are more evident for fibers which are almost completely debonded which display a distinct low frequency resonance, analogous to the Helmholtz resonance of an acoustical cavity. The resonance frequency decreases to zero according to the asymptotic estimate (66) for small neck width. The existence of the resonance phenomenon is significant since its excitation leads to dynamic enhancement of the stress intensity factor, with a correspondingly greater possibility of catastrophic debonding.

References

Abramowitz, M. and I.A. Stegun (1965), Handbook of Mathematical Functions, Dover, New York.

Aveston, J., G.A. Cooper and A. Kelly (1971), Single and multiple fracture, in: The Properties of Fibre Composites, Conference Proceedings, National Physical Laboratory, Guildford, U.K., IPC Science and Technology Press Ltd, p. 15. Budiansky, B., J.W. Hutchinson and A.G. Evans (1986), Matrix fracture in fiber-reinforced ceramics, J. Mech. Phys. Solids 34, 167.

Clemmow, P.C. (1953), Radio propagation over a flat Earth across a boundary separating two different media, *Proc. R. Soc. A 246*, 1.

Cox, H.L. (1952), The elasticity and strength of paper and other fibrous materials, British J. Appl. Phys. 3, 72.

England, A.H. (1976) Complex Variable Methods in Elasticity, Wiley, New York.

Gao, Y.C., Y.W. Mai and B. Cotterell (1988), Elastic fracture mechanics for interfacial cracks, ZAMP 39, 550.

Hashin, Z. and B.W. Rosen (1964), The elastic moduli of fiber-reinforced materials, J. Appl. Mech. 31, 223.

Karihaloo, B.L. and K. Viswanathan (1985), Elastic field of an elliptic inhomogeneity with debonding over an arc (antiplane strain), J. Appl. Mech. 52, 91.

McCartney, L.N. (1989), New theoretical model of stress transfer between fibre and matrix in a uniaxially fibre-reinforced composite, Proc. R. Soc. A 425, 215.

Norris, A.N. and Y. Yang (1990), Dynamic stress on a partially bonded fiber, J. Appl. Mech., in press.

Rice, J.R. (1988), Elastic fracture mechanics for interfacial cracks, J. Appl. Mech. 55, 98.

Sigl, L.S. and A.G. Evans (1989), Effects of residual stress and frictional sliding on cracking and pull-out in brittle matrix composites, Mech. Mater. 8, 1.

Tamate, O. and T. Yamada (1969), Stress in an infinite body with a partially bonded circular cylindrical inclusion under longitudinal shear, Technology Reports, Tohoku University 34, 161.

Yang, Y. and A.N. Norris (1990), Shear wave scattering from a debonded fibre, J. Mech. Phys. Solids, in press.

Appendix A

The rate of working of the time harmonic force $\hat{P}(\omega)$ acting on the fiber r < a, when averaged over a cycle, is

$$\frac{1}{2} \operatorname{Re} \left(\frac{\overline{P(\omega)}}{\pi a^2} (-i\omega) \int_0^{2\pi} d\theta \int_0^a r \, dr \, \hat{u}_f(r, \theta, \omega) \right)$$

$$\equiv R(\omega). \tag{A1}$$

The integral of \hat{u}_f can be performed using (41), and the result simplified by elimination of F_0 in favor of β_0 from (46) and (52). The final form for the power input is

$$R(\omega) = \frac{-\omega |\hat{P}(\omega)|^2}{2\pi\mu_I (k_I a)^2} \text{Im}[\beta_0(\omega)]. \tag{A2}$$

Assuming there is no intrinsic damping in the fiber or matrix, the energy put into the fiber is lost through radiation in the matrix. The balance of energy requires that R is identical to the radiated power, which may be calculated as the integral of the energy flux across any surface enclosing the fiber. The latter can be simply evaluated by using the farfield expansion of $\hat{u}_{\rm m}$, and the energy balance then reduces to the following expression,

$$R(\omega) = 4\omega\mu_{\rm m} \sum_{n=0}^{\infty} \frac{|E_n|^2}{\epsilon_n}, \tag{A3}$$

where E_n are defined in (42). These follow from (44), (46) and (52) as

$$E_{n} = \frac{(-1)^{n} \epsilon_{n}}{2 \pi \mu_{f}} \frac{\rho_{f}}{\rho_{m}} \frac{k_{m}}{k_{f}} \frac{\hat{P}(\omega)}{k_{f} a H_{n}^{(1)'}(k_{m} a)}$$

$$\times \sum_{p=0}^{\infty} J_{2p}(n \epsilon) \beta_{p}(\omega). \tag{A4}$$

The energy balance (A2) can therefore be cast as a relation between the coefficients β_n , $n = 0, 1, 2, \ldots$

$$-\operatorname{Im} \beta_{0}(\omega) = \frac{2}{\pi} \frac{\rho_{f}}{\rho_{m}} \sum_{n=0}^{\infty} \frac{\epsilon_{n}}{|H_{n}^{(1)}(k_{m}a)|^{2}} \times \left| \sum_{p=0}^{\infty} J_{2p}(n\epsilon) \beta_{p}(\omega) \right|^{2}.$$
 (A5)

Appendix B

The restraining stresses in the fiber and matrix for the perfectly bonded fiber of Fig. 8 are related to σ_t^0 by

$$\begin{split} & \sigma_{\rm f}^0 - \sigma_{\rm f}^\infty \\ & = \frac{1 - f}{f} \sigma_{\rm m}^\infty \\ & = \left(\frac{E_{\rm m} + f(\nu_{\rm m} - \nu_{\rm f}) \nu_{\rm m} E_0}{E_{\rm m} + \left[f / (1 - f) \right] E_{\rm f} + f(\nu_{\rm m} - \nu_{\rm f})^2 E_0} \right) \sigma_{\rm f}^0, \end{split}$$
(B1)

where

$$E_0 = 4\left(\frac{1}{\mu_{\rm m}} + \frac{1 - 2\nu_{\rm m}}{\mu_{\rm m}}f + \frac{1 - 2\nu_{\rm f}}{\mu_{\rm f}}(1 - f)\right)^{-1},$$
(B2)

where $f = a^2/b^2$. Noted that (B1) simplifies to an expression given by Sigl and Evans (1989) where $\nu_m = \nu_t$.

The function S(z) of Eqs. (67) and (68) follows from McCartney (1989) as the solution to

$$a^4 \frac{d^4}{dz^4} S(z) - 2a_1 a^2 \frac{d^2}{dz^2} S(z) + b_1^2 S(z) = 0,$$
(B3)

subject to the restraints upon S(z) that it and its derivative should vanish as $z \to \infty$, while at z = 0 the pull-out load on the fiber is assumed to be purely axial, see Fig. 8. Thus,

$$\sigma_{rz}^{f} = 0, \quad \sigma_{rz}^{f} = \sigma_{f}^{0}, \quad z = 0,$$
(B4)

implying

$$S'(0) = 0, \quad S(0) = \sigma_f^0 - \sigma_f^\infty,$$
 (B5)

Note that these end conditions automatically imply that $\sigma_{zz}^{m}(0) = 0$. The solution for S(z) is (McCartney, 1989)

$$S(z) = S_0 e^{-pz/a}$$

$$\times \begin{cases} \left[\cos(qz/a) + (p/q)\sin(qz/a)\right], \\ a_1 < b_1, \\ (1 + pz/a), \\ a_1 = b_1, \\ \left[(p+q) e^{qz/a} - (p-q) e^{-qz/a}\right]/2q, \\ a_1 > b_1, \end{cases}$$
(B6)

where

$$p = \left[\frac{1}{2}(a_1 + b_1)\right]^{1/2}, \quad q = \left(\frac{1}{2}|a_1 - b_1|\right)^{1/2},$$

$$a_1 = \frac{-G}{2F}, \quad b_1 = \sqrt{\frac{H}{F}}, \tag{B7}$$

and
$$F = \frac{(1 - \nu_f)(1 - f)}{8\alpha E_f E_m f} \left[1 + (1 + \nu_m)I\right] - \frac{1 + \nu_m}{4E_m} \left(I - \frac{1 - f}{2f}\right) \gamma,$$

$$G = \beta \gamma + \frac{(1 - f)\delta}{2fE_f} + \frac{1 + \nu_m}{E_m} \frac{\beta}{\alpha} \left(I - \frac{1 - f}{2f}\right) + \frac{1}{2}(1 - f) \left(\frac{1}{E_m} - \frac{1}{E_f}\right) - \left(\frac{1 + \nu_m}{E_m} - \beta\right)I,$$

$$H = \frac{2f}{E_m} + \frac{2(1 - f)}{E_f} - \frac{4\beta^2}{\alpha},$$

$$I = \frac{1}{1 - f} \log\left(\frac{1}{f}\right) - 1,$$

$$\alpha = \frac{1 + \nu_m}{E_m} + \frac{1 - \nu_m}{E_m} f + \frac{1 - \nu_f}{E_f} (1 - f),$$

$$\beta = \frac{\nu_m}{E_m} f + \frac{\nu_f}{E_f} (1 - f),$$

$$\gamma = \frac{1}{\alpha E_m} - \frac{1}{2} + \left(\frac{1 + \nu_m}{\alpha E_m} - 1\right)I,$$

$$\delta = \nu_f - (1 - \nu_f) \frac{\beta}{\alpha}.$$

McCartney (1989) reports that exhaustive numerical computations for a range of material parameters indicate both a_1 and b_1 are positive.

We note that the location of maximum stress gradient occurs where $\partial \sigma_{zz}^f/\partial z$ is minimum, or equivalently, where S'(z) has a minimum. This is also the point at which the shear stress σ_{rz}^f is maximum. From (B6) we deduce the location as the root of

$$\begin{split} \tan\!\left(\frac{qz}{a}\right) &= \frac{q}{p}\,, \qquad a_1 < b_1\,, \\ \frac{z}{a} &= \frac{1}{p}\,, \qquad a_1 = b_1\,, \\ \tanh\!\left(\frac{qz}{a}\right) &= \frac{q}{p}\,, \quad a_1 > b_1\,. \end{split} \tag{B8}$$

If $a_1 < b_1$, the desired value of z is the smallest positive root.